

Design and experimental analysis of an Integral Collector Storage (ICS) prototype for DHW production

Original

Design and experimental analysis of an Integral Collector Storage (ICS) prototype for DHW production / Bilardo, M.; Fraisse, G.; Pailha, M.; Fabrizio, E.. - In: APPLIED ENERGY. - ISSN 0306-2619. - ELETTRONICO. - 259:114104(2020). [10.1016/j.apenergy.2019.114104]

Availability:

This version is available at: 11583/2780454 since: 2020-01-15T12:15:22Z

Publisher:

Elsevier Ltd

Published

DOI:10.1016/j.apenergy.2019.114104

Terms of use:

openAccess

This article is made available under terms and conditions as specified in the corresponding bibliographic description in the repository

Publisher copyright

Elsevier postprint/Author's Accepted Manuscript

© 2020. This manuscript version is made available under the CC-BY-NC-ND 4.0 license
<http://creativecommons.org/licenses/by-nc-nd/4.0/>. The final authenticated version is available online at:
<http://dx.doi.org/10.1016/j.apenergy.2019.114104>

(Article begins on next page)

Pre-print version of:

Bilardo, M., Fraisse, G., Pailha, M., & Fabrizio, E. (2019). Design and experimental analysis of an Integral Collector Storage (ICS) prototype for DHW production. *Applied Energy*, 114104.

<https://doi.org/10.1016/j.apenergy.2019.114104>

DESIGN AND EXPERIMENTAL ANALYSIS OF AN ICS PROTOTYPE FOR DHW PRODUCTION

Matteo Bilardo^{2,*}, Gilles Fraisse¹, Mickael Pailha¹, Enrico Fabrizio²

¹*Univ. Grenoble Alpes, Univ. Savoie Mont Blanc, CNRS, LOCIE, 73000 Chambéry, France*

²*Politecnico di Torino. DENERG – Department of Energy, Corso Duca degli Abruzzi, 24, 10129 Torino, Italy*

*Corresponding author: matteo.bilardo@polito.it

Abstract

This paper presents an innovative solar ICS (integral collector storage) for the production of domestic hot water (DHW). The novelty consists in combining an absorbent surface, heat pipes and a storage cavity made up of a phase change material (PCM) within a single compact casing. The energy performance of the system was experimentally studied in different seasons of the year, with and without domestic hot water production. The temperatures inside the collector were monitored using special thermocouples and their trends were analysed and discussed. During the experimental phase, the thermal storage reached the maximum temperature of 79.3 °C, exploiting the latent heat of the PCM. Overall performances demonstrated good agreement with results available in the literature in terms of efficiency and energy storage. A specific heat flux of 2.64 kW.m⁻² was achieved in DHW production, with a water flowrate of 0.87 kg.min⁻¹. The 0.02 m³ PCM section was able to store 24.57 kWh of thermal energy along a monitored month. Future developments of this new technology include new experimental tests with larger prototypes and the coupling with a real user.

Nomenclature

Abbreviations

ICS	Integral collector storage
PEG	Polyethylene glycol
HP	Heat pipe
DHW	Domestic hot water
TES	Thermal energy storage
HTF	Heat transfer fluid

Variables

c_p	Specific thermal capacity (J.kg ⁻¹ .K ⁻¹)
C	Thermal capacity (J.K ⁻¹)
E	Solar radiation (W.m ⁻²)

Pre-print version of:

Bilardo, M., Fraisse, G., Pailha, M., & Fabrizio, E. (2019). Design and experimental analysis of an Integral Collector Storage (ICS) prototype for DHW production. Applied Energy, 114104.

<https://doi.org/10.1016/j.apenergy.2019.114104>

D	Global heat transfer coefficient ($\text{W}\cdot\text{m}^{-2}\cdot\text{K}^{-1}$)
A	Area (m^2)
T	Temperature (K)
U_{HP}	Heat transfer coefficient for one heat pipe ($\text{W}\cdot\text{K}^{-1}$)
\dot{Q}_{sto}	Stored heat (W)
\dot{Q}_{HP}	HP transferred heat (W)
\dot{Q}_{loss}	Lost heat (W)
\dot{Q}_{DHW}	Power extracted by the water (W)
η	Efficiency (-)
\dot{m}_w	Water flow rate ($\text{kg}\cdot\text{s}^{-1}$)
<i>Indices</i>	
abs	Absorber
eva	Evaporator
cond	Condenser
pe	Front cavity plate
pi	Back cavity plate
ext	External
in	Inlet
out	Outlet

1 Introduction

The total world consumption of primary energy is constantly increasing. However, the percentage of primary energy globally produced from renewable sources only reaches 10.4%, while the largest energy share (79.5%) is still produced through the exploitation of fossil fuels [1]. For this reason, the research and development of new technologies able to make the most of renewable resources has assumed a fundamental role in recent years. The lack of energy production from existing renewable energy sources has a negative impact on the environment, demonstrated by the constant increase in CO₂ emission [2]. To cope with these problems, most governments are imposing directives to steer their states towards energy sustainability and energy transition. Already in 2007, the leading European countries set targets for 20/20/20, in terms of emissions, energy consumption and use of renewable sources [3]. Although now close to achieving this goal, the European directive has already imposed a decarbonisation plan that by 2050 provides for the reduction of greenhouse gasses by 80-95% compared to the values recorded in 1990 [4].

Space heating and cooling in buildings is the sector with the largest energy consumption, holding a 48% share. This share is roughly split equally between the industrial and residential sectors [5]. Residential buildings are some of the main energy consumers and are consequently responsible for the production of atmospheric pollutants, such as carbon dioxide [6]. The integration of technologies based on renewable sources within buildings is now an established technology in the vast majority

Pre-print version of:

Bilardo, M., Fraisse, G., Pailha, M., & Fabrizio, E. (2019). Design and experimental analysis of an Integral Collector Storage (ICS) prototype for DHW production. *Applied Energy*, 114104.

<https://doi.org/10.1016/j.apenergy.2019.114104>

of European countries, where a percentage of the energy consumption of each new building must be covered by renewable sources. With the RT2012 regulation, France requires that all new buildings should have an average energy consumption lower than 50 kWh/m² per year of primary energy, and also obliges all single-family houses to have renewable plants integrated with traditional systems of energy production [7]. Likewise in Italy, Legislative Decree 28/2011 provides that starting from 2018 new buildings have a minimum share of primary energy production from RES equal to 50% [8]. Similar regulations have been adopted in other European countries, and almost all national regulations refer to and implement the European Energy Performance of Building Directive (EPBD), which provides guidelines on how to support the energy needs of buildings in order to meet and reach common objectives imposed by the 20/20/20 targets [3]. Recently the European Union established a recast of the EPBD directive, promoting a clean energy transaction in line with its commitment to reduce CO₂ emissions by at least 40% by 2030 [9]. This process of decarbonisation, that heavily involves the construction sector, also has as its objective the development of new buildings closer to the nZEB model [10]. The EPBD directive has promoted considerable growth and innovation in recent years both in the construction of new buildings and in the field of scientific research, where several studies regarding new technological solutions, as well as optimization processes, have been carried out [11,12].

Traditional energy production systems are now always integrated with renewable sources inside buildings [13]. The majority of the solutions include the installation of photovoltaic panels, aimed at the production of electricity, or of solar collectors for the production of thermal energy. The installation of solar thermal panels is now a consolidated process in building works and involves the coupling of solar collectors with a water-based thermal storage system, which is then integrated with a traditional system [14]. This setup is usually composed of a collector-storage-plant system and is certainly the most widespread and the most economically feasible.

Solar thermal collectors used in buildings are usually stationary and can be grouped into three main categories: flat collectors, vacuum tubes and compound parabolic collectors. The first two categories represent approximately 93.2% of the collectors installed in the world [15], and are therefore the most currently adopted technologies on the market. In China, that is the first country in the world for installed solar thermal power, most of the installations are made of evacuated tube collectors. By contrast, in Europe the preferred choice is flat plate collectors [16]. From 2014 the growth rate of installed solar thermal power compared to the previous year has become negative, indicating a predictable market saturation by current technologies. On the other hand, thermal storage market is constantly increasing, and future forecasts indicate a further growth of this sector [17,18]. It is therefore evident that the attention of the market is shifting more and more towards efficient methods of storing energy produced from renewable sources [19,20]. In this context, many studies have researched new innovative thermal storage systems [21,22]. What usually characterizes the storage systems is the thermal capacity of the material used, which determines

Pre-print version of:

Bilardo, M., Fraisse, G., Pailha, M., & Fabrizio, E. (2019). Design and experimental analysis of an Integral Collector Storage (ICS) prototype for DHW production. *Applied Energy*, 114104.

<https://doi.org/10.1016/j.apenergy.2019.114104>

the amount of heat that the material is able to store. The heat exchange capacity should also be as high as possible, in order to maximize not just the thermal exchange rate between the storage and the heat transfer fluid (HTF) but also between the storage and the cold sanitary water in the case of SDHW, where higher power is involved in the heat extraction from the storage rather than in the storage charging process. In addition, mechanical and chemical stability must be tested to avoid the degradation of the material, especially when it is subjected to numerous cycles of thermal loading and discharge. Finally, the economic aspect must be taken into consideration.

Possible storage systems can be grouped depending on the mechanism by which the energy is stored [23,24]. In addition to the sensible heat, phase change materials (PCM) exploit the latent heat during a state change in order to increase the storage capacity without increasing their temperature. Storages based on PCM have a higher energy density compared with water-based storages that work in a limited range of temperature and they can accumulate and provide energy in a smaller thermal rise or drop [25]. Due to the growing diffusion, in the next few years a significant reduction in the price of PCM is expected, thus encouraging their marketing on a larger scale [26].

The transfer of the heat collected by the solar collectors towards a thermal storage is another fundamental aspect of these systems. Among the devices that perform this task, heat pipes are an excellent solution both for thermal performance and for their passive operation [27]. The application of heat pipes in solar collectors can lead to innovative and energy-efficient solutions [28]. A more detailed examination of these systems is given in the following section.

1.1 Use of PCM and heat pipes on ICS applications

In the framework that has been presented, Integral Collector Storages (ICS) represent an interesting object of study with possible economic impact on the market. This category of solar collectors allows to solve most of the problems related to traditional systems. In the past years, several research projects focused ICS, offering different technical solutions. A careful review of the fundamental principles underlying the operation of an ICS was conducted by Smyth et al. [29], who have reviewed the progresses made in the experimental field. It is certain that the use of heat pipes and phase change materials as integral elements of a solar collector is not entirely new. In the past few decades several experimental studies have been conducted trying to implement these technologies in the field of solar thermal. Already in 2001 a study conducted by Susheela et al. [30] demonstrated the effectiveness of the use of heat pipes integrated into the walls of a building, connecting an absorber surface installed on the external wall facing south with a water storage tank. The solar heat, removed from the heat pipes, is transferred to the water storage, positioned in an internal environment. Through a natural convection exchange mechanism, the storage tank is free to release heat to the internal environment, shifting the peak of solar energy. This solution belongs to passive heating systems and includes the implementation of heat pipes that perform the function of thermal diodes,

allowing the heat to flow only in one direction, thanks to the slight inclination upwards. A continuous passage of state of the HTF through evaporation and condensation processes occurs inside the heat pipe: in this way the heat flow is forced to flow in a preferential direction, as shown in Fig. 1a. A system implementing this technology was designed and subsequently verified by Robinson et al. [31] (Fig. 1b), which demonstrated an average daily thermal efficiency of 61.4% during an entire heating season in a humid subtropical climate. The same author also identified the possible drawbacks that this system can cause. In the experiment analysed, the effect of thermal diode performed by the heat pipes generates a positive effect in terms of thermal gains during the winter period, while causes a sharp increase in cooling loads during the summer since the heat flux cannot pass through the heat pipe in the opposite direction.

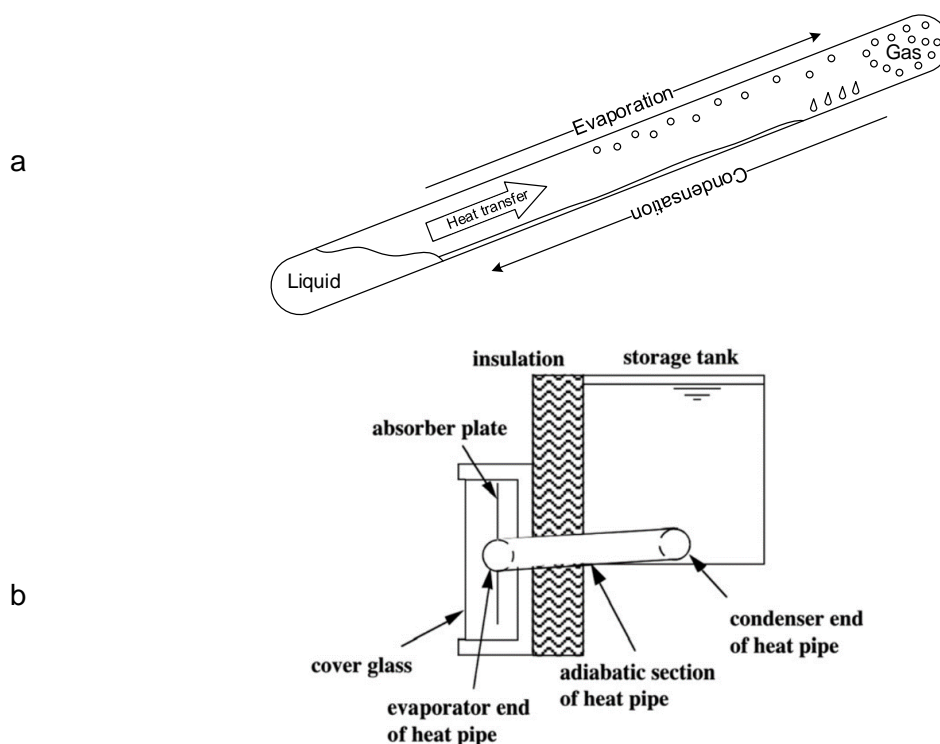


Fig. 1. Heat pipe operating principle (a) and 2D schematic of unit studied by [31] (b)

To counteract this negative effect, Robinson et al. [32] experimented several possible solutions, testing both design modifications (implementing solar shadings) and control strategies achieving the optimal results to limit the cooling loads due to the heat pipe walls. However, the use of heat pipes in solar systems remains an advantageous method with great potential from an energy point of view. Some of the energy evaluation parameters defined and adopted by Robinson have been implemented into the research work reported in this paper, having the two systems particular similarities. Another study concerning the application of heat pipes, conducted by Esen et al. [33], tested the thermal performance of a two-phase thermosyphon solar collector. This collector takes

Pre-print version of:

Bilardo, M., Fraisse, G., Pailha, M., & Fabrizio, E. (2019). Design and experimental analysis of an Integral Collector Storage (ICS) prototype for DHW production. *Applied Energy*, 114104.

<https://doi.org/10.1016/j.apenergy.2019.114104>

advantage of the use of heat pipes to transport solar energy to a water storage tank located in the upper part of the system (Fig. 2).

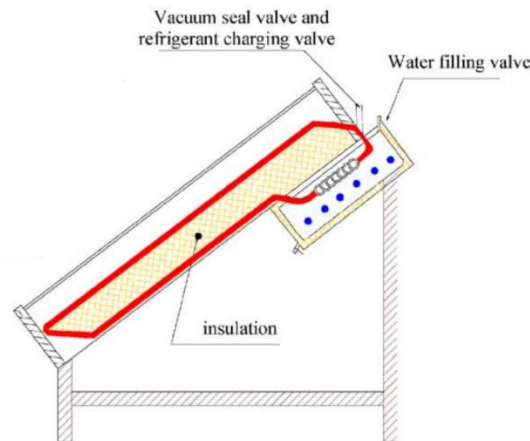


Fig. 2. Experimental set-up of thermosiphon two-phase solar collector studied by [33]

In the experiment conducted by Esen heat pipes work thanks to the effect of gravity, being installed with the condenser installed in a higher position with respect to the evaporator. This solution generates a passive two-phase thermosiphon system that does not require the installation of auxiliary elements. The purpose of the author's research was a peculiar study on how different refrigerant fluids that are used as heat transfer fluids inside the heat pipes might affect the heat capacity of the collector. Besides providing some guidelines in the selection of a specific fluid for the heat pipe, the results of the study demonstrated the reliability of an integrated storage system obtaining efficiencies comparable with other solutions on the market.

In addition to heat pipes in solar thermal systems, the adoption of PCM has recently gained some interest in solar thermal installations. The use of PCMs is becoming increasingly common in energy applications related to solar energy, mainly for two reasons. Firstly, exploiting the latent heat of phase change, a PCM is able to store large amounts of energy without involving high temperature rises. Secondly, PCMs have a higher energy density than traditional materials, thus leading to savings in terms of volume occupied [34]. A valid review of the state of the art regarding the applications of PCMs in solar thermal technologies is provided by Sadhishkumar et al. [35]. In this review, several possible implementations of PCMs are underlined. Vikram et al. [36] demonstrated how PCMs are reliable to make the solar thermal energy available at night and Anant et al. [37] indicate how they can be involved in systems that include a traditional water storage section, concluding that latent heat storage is a commercially viable option.

Various application possibilities of PCMs have been summarized by Kousksou et al. [38], which indicates three main scenarios involving PCMs within a solar thermal system

Pre-print version of:

Bilardo, M., Fraisse, G., Pailha, M., & Fabrizio, E. (2019). Design and experimental analysis of an Integral Collector Storage (ICS) prototype for DHW production. *Applied Energy*, 114104.

<https://doi.org/10.1016/j.apenergy.2019.114104>

- Integrated PCM inside a storage tank that separates a primary circuit (solar loop) from a secondary (user loop) (Fig. 3a);
- PCM included in the primary circuit as an additional storage system (Fig. 3b);
- Integrated PCM inside the collector (ICS with PCM) (Fig. 3c).

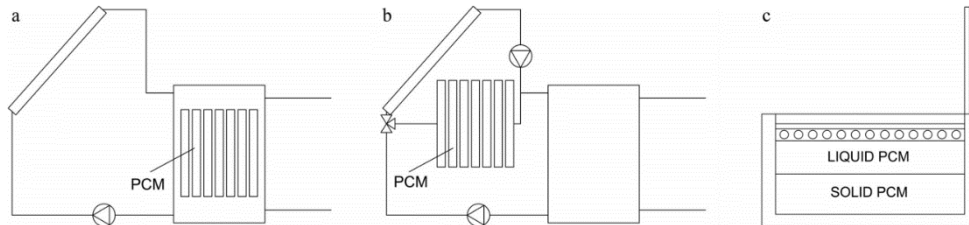


Fig. 3. Examples of PCM integration into solar thermal systems [39]

A further technical solution has been realized and studied by Serale et al. [39], proposing a system composed of an open primary loop where microencapsulated phase change slurry (mPCS) has been adopted (Fig. 4). This slurry is a mixture of microencapsulated phase change material, water and surfactants and was used as heat transfer fluid (HTF). The open primary loop also integrates the storage tank. In this specific experiment, the HTF coincides with the energy storage medium. A closed secondary loop was in charge of extracting heat from the storage tank and distribute it towards a possible user.

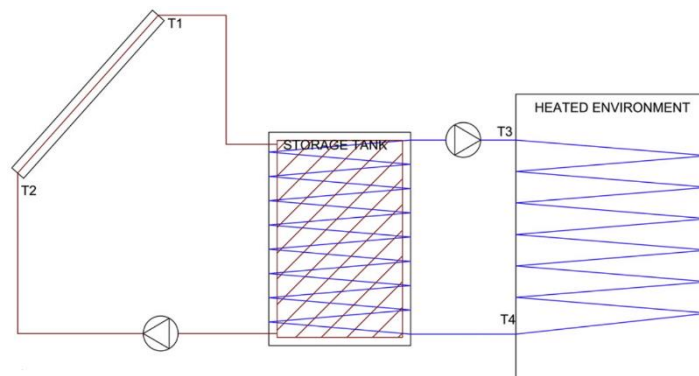


Fig. 4. Schematics of the prototype studied by [39]

Results from this set up showed that the use of mPCS as HTF is promising, especially for low temperature applications (about 40°C). However, the system presents some technical issues related to the stratification of the HTF in the storage tank that, when not subjected to continuous mixing, it risks of incurring into the separation between the mPCS and the other components of the slurry solution.

Another innovative design was proposed by Hailiot et al. [40]. After studying the properties of different composites made of compressed expanded natural graphite (CENG) and various PCMs (paraffins, sodium acetate, ...), the authors designed an ICS composed of a flat plate collector with

Pre-print version of:

Bilardo, M., Fraisse, G., Pailha, M., & Fabrizio, E. (2019). Design and experimental analysis of an Integral Collector Storage (ICS) prototype for DHW production. *Applied Energy*, 114104.

<https://doi.org/10.1016/j.apenergy.2019.114104>

a CENG/PCM storage section in direct contact with the absorber. The collector was then placed inside a casing made from a polymer (Fig. 5).

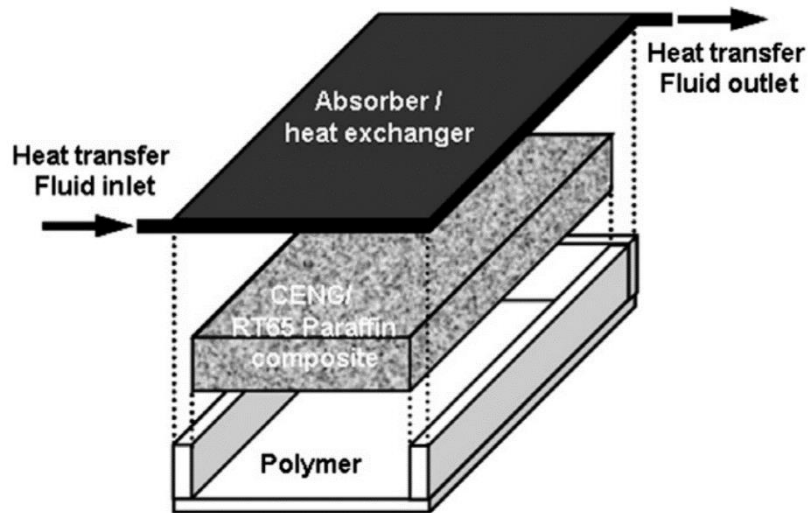


Fig. 5. ICS-CENG/PCM design [41]

The originality of this application consists in the fact that the traditional storage tank, a typical component in the majority of solar domestic hot water (SDHW) systems, is completely removed. Instead, the PCM compound has been placed directly on the backside of the absorber, designing both the solar absorber and the storage section in a very limited thickness. The experimental phase of this project was followed by the development of a numerical model, which was validated with experimental data [41].

Further experimental studies on ICSs, although not directly involving the use of PCM or heat pipes, have been carried out by Souza et al. [42]. The authors have in fact studied in depth the behaviour of a thermal storage cavity positioned on the back of an absorber. By simulating the solar radiation variability using a heating plate with the same thermal properties as solar radiation, they succeed in studying the energy responses of the storage section, particularly focusing on thermal stratification and convective thermal exchange. In the experiment conducted, the storage medium used was distilled water. The results obtained showed unsatisfactory thermal stratification, with a limited temperature difference between the upper and the lower part of the cavity, demonstrating the need of an additional element capable of promoting the stratification process. The experiment therefore proved how the use of ICSs often requires implementations that are slightly different from the traditional ones. The positioning and design of the storage section, which into an ICS must be an integral part of the collector, require particular attention and must guarantee not only an efficient heat transfer, but also addressable problems related to the spatial placement of the internal elements.

Pre-print version of:

Bilardo, M., Fraisse, G., Pailha, M., & Fabrizio, E. (2019). Design and experimental analysis of an Integral Collector Storage (ICS) prototype for DHW production. *Applied Energy*, 114104.

<https://doi.org/10.1016/j.apenergy.2019.114104>

1.2 Aim of the study

In this work, the findings from an experimental investigation on an innovative ICS prototype for the production of domestic hot water are reported. The technological innovation proposed by this new concept is based on the integration of the heat pipes, used as heat flux carrier, with a PCM-based storage. These two elements, unconventional for the standard solar collectors available on the market, are coupled in the same device, providing at the same time an insulated solar circuit and a storage section. The aim of the following study is to validate the functioning and competitiveness of the prototype with respect to traditional solutions. This innovative system aims to pursue the following objectives:

- **Easy installation**
The prototype is as an integrated system that does not need auxiliaries, such as circulation pumps and electrical components. The storage section is enclosed inside the same casing of the absorber, generating a different design from traditional systems, where the storage is usually detached from the absorber. Being completely insulated from the external environment, the whole system is designed to be installed outdoors, without requiring special structural alteration.
- **Passive functioning**
An advantage of the proposed system is that of being able to operate in a passive way, reducing maintenance operations to a minimum impact. The system is designed to work autonomously without manual control operations, providing, when requested by the user, a source of domestic hot water. The prototype can be coupled with a traditional system, providing an additional source of renewable energy.
- **Energy efficiency**
The system has been designed to achieve results in terms of energy efficiency similar to solution available on the market, especially for installations aimed at harsh climates.

The studies related to the ICS prototype can be divided into three main stages: in the first preliminary stage the prototype was designed and then commissioned. Every single functional element was produced and assembled to create a first operating prototype. A second stage was therefore focused on the experimental study of the energy performance, submitting the prototype to a series of cycles of standard operation, as well as to domestic hot water collection tests. Finally, a third stage of study, which was developed simultaneously with the stages one and two, aimed to the development of a mathematical model able to simulate the physical behaviour of the ICS prototype. The detailed numerical study of the prototype is outside the scope of this paper and has been addressed in a dedicated study [43]. However, the prototype design process and the collection of experimental data, object of the study contained in this paper, were fundamental for the development and the validation of the numerical model.

2 Prototype design

The designed ICS prototype was developed within the Université Savoie Mont Blanc (USMB) campus and funded by Agence De l'Environnement et de la Maitrise de l'Energie (ADEME) (see acknowledgements). Fig. 6 shows the prototype scheme, visualizing the internal components position. The novelty of this ICS is to combine within a single casing the following elements:

- Collector section composed by a glass coverage, an air gap and the flat-plate absorber layer;
- Heat pipe section, connecting the absorber to the storage;
- Storage cavity made up of honeycomb cells filled by PCM;
- Insulation layer all around the storage section.
- DHW heat exchanger, welded to the front side plate of the cavity.

What makes this prototype unique is the heat transfer mechanism from the flat-plate absorber and the storage section: between these two elements six heat pipes were designed and filled with methanol, which acts as HTF. The task of the heat pipes is to thermally decouple the absorber from the storage, removing the heat absorbed and transferring it towards the storage cavity containing the PCM. Heat pipes, designed to operate in natural convection conditions, are installed with a slight inclination (5°). In addition to enabling heat transfer, the heat pipes therefore perform as thermal diode, in order to insulate the cavity. The cavity containing PCM has been designed as thermal energy storage and it is positioned on the back of the collector. Polyethylene glycol 6000 (PEG 6000) is the phase change material that has been chosen. Finally, domestic hot water is produced instantaneously by means of a copper coil that wraps around the storage section.

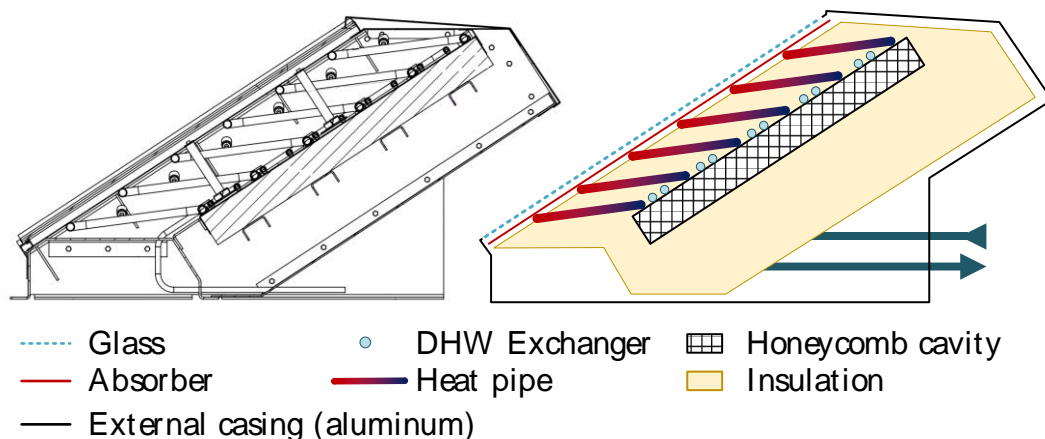


Fig. 6. Prototype main internal components

Pre-print version of:

Bilardo, M., Fraisse, G., Pailha, M., & Fabrizio, E. (2019). Design and experimental analysis of an Integral Collector Storage (ICS) prototype for DHW production. *Applied Energy*, 114104.

<https://doi.org/10.1016/j.apenergy.2019.114104>

The prototype examined is unique and not yet intended for the commercial market. Since the study was carried out in a laboratory environment and subsequently validated in an outdoor environment, the technology readiness level can be estimated at 5 [44].

2.1 Principle of operation

For a better understanding on how the collector works, the solar energy flow can be considered referring to Fig. 7 and Fig. 8. Solar radiation hits the front face of the collector, consisting of a simple flat-plate absorber section with a glass cover, commonly used by standard systems. Absorber converts solar energy into thermal power, that is immediately released to the heat pipe section which makes contact with the back side of the absorber. Once solar energy reaches the heat pipe section, energy is transferred to the heat transfer fluid (HTF), i.e. methanol. Heat pipes are in fact made with U-shaped copper tubes, hermetically sealed and filled for 30% of their volume with methanol. Liquid methanol settles on the lower part of the heat pipe, right behind the absorber. Thermal heat transferred from the absorber makes the methanol evaporates. Gaseous methanol is now free to move towards the highest section of the heat pipe, where it faces the colder storage cavity wall and condensates, reaching again the liquid state and flowing back to the lowest section. The general heat pipe working principle is shown in Fig. 1a. Two main segments inside the heat pipe can be distinguished: the evaporator section, behind the absorber and the condenser section, next to the storage cavity. Fig. 7 points out the energy loop that occurs inside the heat pipe, where the heat carrier is the methanol. Such solution makes advantage of the heat pipe slope to create a classical thermosiphon heat cycle based on natural convection driven just by gravity, that does not need any auxiliary equipment such as a circulation pump. Furthermore, the benefit of such solution is to allow the heat flux to flow only in one direction, from the evaporator to the condenser, to maximize the effect of the incident solar radiation on the absorber and avoiding energy losses due to a reverse energy flow. Finally, the process does not include any control device and the heat flow that passes through the heat pipe is proportional to the temperature difference established between the evaporator and the condenser.

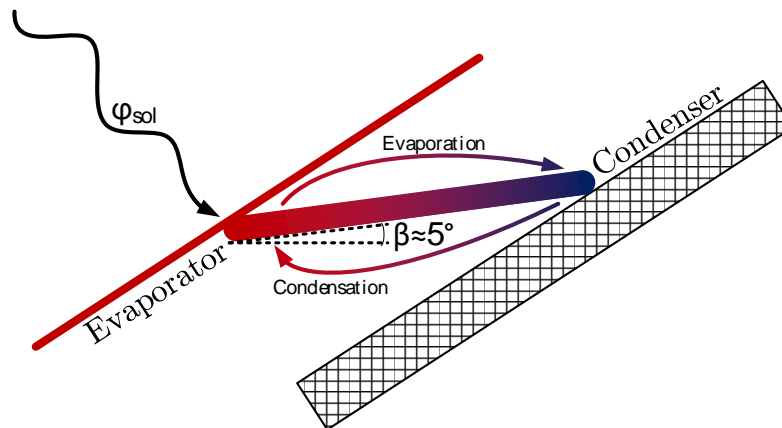


Fig. 7. Heat pipe energy loop

After passing through the heat pipe and reaching the condenser, the energy flows inside the aluminium cavity and heats the PCM up. The heat exchange occurs on the cavity front plate, where the condenser section is welded. The PCM temperature starts increasing until it reaches the double phase region, initiating the melting process (from 50 °C to 55 °C). Regarding the phase change material, polyethylene glycol (PEG) was adopted because of its advantageous thermo-physical properties, which will be addressed in the next section of the paper. PEG was placed inside the honeycomb cells of the cavity with a filling rate of 75% in volume that allows the material to expand during the phase change without compromising the mechanical stability of the structure. The honeycomb pattern is kept in position by two aluminium plates on both sides. Once the energy is stored in the PCM, it is ready to be supplied to a hydraulic circuit in order to provide domestic hot water (DHW) to a possible user. A new energy loop is therefore introduced into the system, consisting of a DHW pipeline installed in the same position of the heat pipe condenser, on the cavity front side. This strategic placement provides a double advantage from an energy point of view: on one hand it allows the cavity to discharge energy on the DHW pipeline, on the other it makes available a direct energy transfer from the condenser to the DHW pipeline, avoiding the energy storage step. This last scenario might be useful when the heat production matches the hot water demand: in this case the heat flowing through the heat pipe can be directly discharged towards the DHW pipeline, since the HP condenser and the DHW exchanger are welded on the same plate (aluminium cavity front plate). The heat exchange is therefore predominantly conductive through the cavity front plate. For this study purposes, cold water from the network is intended to flow inside the DHW pipeline, made by a simple copper pipe. When the user needs it, a certain water flow goes through the pipe increasing its temperature.

To summarize, when considering the interface between heat pipes and storage cavity, four energy fluxes are involved in the prototype principle of operation (Fig. 8):

- 1) Φ_1 : Heat flow through the heat pipes, with methanol as heat carrier (\dot{Q}_{HP});

Pre-print version of:

Bilardo, M., Fraisse, G., Pailha, M., & Fabrizio, E. (2019). Design and experimental analysis of an Integral Collector Storage (ICS) prototype for DHW production. *Applied Energy*, 114104.

<https://doi.org/10.1016/j.apenergy.2019.114104>

- 2) Φ_2 : Heat flow from the condenser to the PCM, charging the storage;
- 3) Φ_3 : Heat flow from the PCM to the DHW, discharging the storage;
- 4) Φ_4 : Direct heat flow from the condenser to the DHW, bypassing the PCM

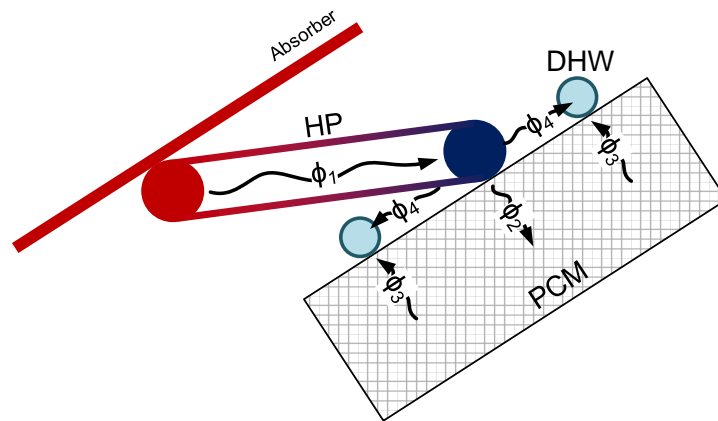


Fig. 8. Principe of operation and main heat fluxes

Moreover, three different heat carriers/storage media are involved in the system:

- 1) Methanol inside the heat pipes, transferring solar radiation from the absorber to the cavity and acting as a thermal diode;
- 2) PEG inside the aluminium cavity, as a storage medium;
- 3) Water in the DHW pipeline, extracting the energy produced and stored in the collector.

Comparing it with traditional solar thermal systems, this new ICS concept makes it available a stand-alone installation with no needs of external equipment. This prototype wants to introduce a simple and effective solution for DHW production with solar energy, taking advantage of its simple installation, good architectural integration and appropriate insulation to avoid freezing risks in the water loop, especially in harsh climates. Being completely isolated, the water used for domestic purposes is not intended to be treated and can flow directly into the DHW exchange coil of the ICS. Moreover, in conditions of non-demand from the user, the risk of freezing is avoided since the thermal storage discharges heat towards the exchange coil, keeping it at the same temperature of the storage. After the literature review, no systems combining heat pipes, fully insulated storage and PCM in a honeycomb structure were found. This will certainly give to the study a unique value for the development of similar technologies.

2.2 Prototype components

The production process allowed the manufacturing of specific components that could not be purchased, so that each element of the prototype was made ad-hoc to perform the function previously established in the design phase. The flat-plate absorber is the only element that belongs to a current model available on the market, manufactured by CLIPSOL [45]. Given the experimental

Pre-print version of:

Bilardo, M., Fraisse, G., Pailha, M., & Fabrizio, E. (2019). Design and experimental analysis of an Integral Collector Storage (ICS) prototype for DHW production. *Applied Energy*, 114104.

<https://doi.org/10.1016/j.apenergy.2019.114104>

purposes, the prototype realized has rather small dimensions, with an opening area of 0.5 m^2 (1 m width and 0.5 m length) and a maximum height of 0.427 m. The absorber slope is set to 33° : this design choice was made in accordance to both the latitude of the installation site and the slope of the heat pipes. The total weight of the prototype, without considering the supporting structure, is around 60 kg.

2.2.1 Honeycomb storage cavity

The cavity that contains the phase change material consists of three elements: two aluminium plates and the honeycombs internal structure. Fig. 9 shows the interior of the cavity, counting on more than 6000 hexagonal shape cells with a frontal section of 0.74 cm^2 and 0.04 m height (Fig. 10). The total volume of the cavity is 0.02 m^3 and the amount of PCM used is 18.15 kg. The specific storage used in the prototype is therefore 0.04 m^3 per each square meters of absorber surface. The entire structure was vacuum-assembled with the aluminium panels, in order to avoid that the material inside could migrate from one cell to another. PEG is therefore able to expand when it melts, without moving from its original cell. In this way, the amount of PCM in each cell it is kept constant during operational condition, giving the cavity a homogeneous thermal and mechanical behaviour.



Fig. 9. Honeycomb structure

Pre-print version of:

Bilardo, M., Fraisse, G., Pailha, M., & Fabrizio, E. (2019). Design and experimental analysis of an Integral Collector Storage (ICS) prototype for DHW production. *Applied Energy*, 114104.

<https://doi.org/10.1016/j.apenergy.2019.114104>

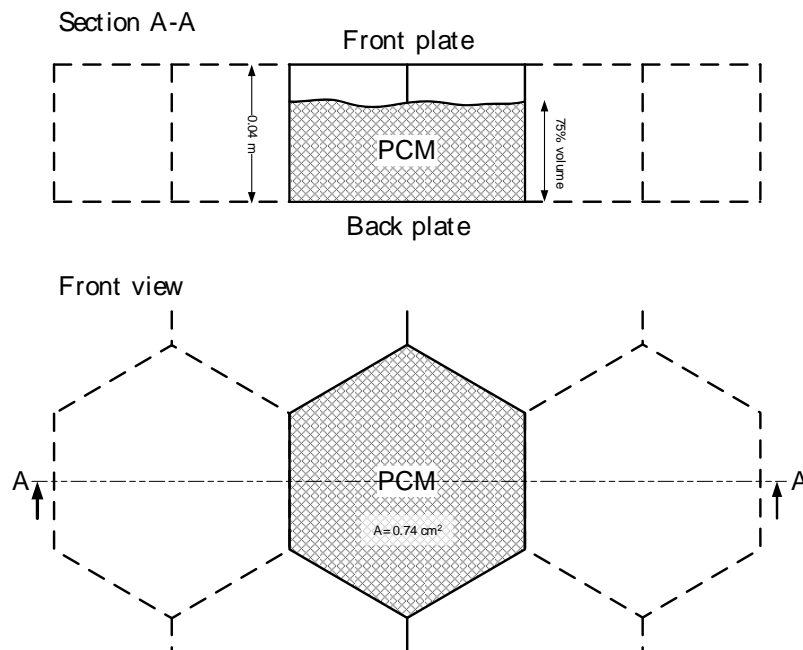


Fig. 10. Honeycomb cell (detail)

The entire storage cavity has been made of aluminium to improve the thermal performances and at the same time limit the weight. The honeycomb shape seemed the best solution to place the PCM in the most uniform possible way and to allow an effective heat exchange between the structure and the aluminium plates. The honeycomb structure was sealed on both sides by welding the two aluminium plates on it so that the PEG cannot move from one cell to another, ensuring a homogeneous thermal behaviour. Once the cavity was manufactured, it is no longer possible to open it without compromising its operation.

2.2.2 Heat pipes

Six heat pipes filled with methanol have been installed in parallel between the absorber and the storage cavity, as shown in Fig. 6. Three main sections can be identified:

- 1) The evaporator, that collects the solar energy;
- 2) The adiabatic heat transfer duct;
- 3) The condenser, that gives back the collected heat to the storage.

The thermal diode effect and the passive functioning are the main advantages that led to the adoption of heat pipe in the prototype. Heat pipes have a U-shape geometry with two long sides (1-meter length) horizontally installed representing the evaporator and the condenser. The short side, about 0.2 m, has a slight slope. The inner diameter is constant, and it is equal to 1 cm. Methanol was chosen as a working fluid because of its physical properties related to the operational temperatures, which can reach 100 °C. At these high temperatures, the operating pressure does not exceed 4 bars. Other fluids considered by Fraisse et al. [46], like ammonia, might reach dangerous

Pre-print version of:

Bilardo, M., Fraisse, G., Pailha, M., & Fabrizio, E. (2019). Design and experimental analysis of an Integral Collector Storage (ICS) prototype for DHW production. *Applied Energy*, 114104.

<https://doi.org/10.1016/j.apenergy.2019.114104>

pressures values at those temperature, compromising the heat pipe functioning. Finally, the choice of methanol made it possible to adopt copper as a construction material, improving sturdiness and ensuring longer life to the component.

2.2.3 DHW exchanger

The DHW exchanger was designed according to the required power output, based on the water temperature increase and the water flow. The exchanger consists of a simple copper pipeline with a total length of 12 meters. Internal and external diameter are respectively 6 and 8 mm. The exchanger pipe was placed alongside the heat pipe condenser, welded on the upper cavity plate to favour the direct heat exchange between the two elements. The domestic hot water piping is the only elements of the system that communicates with the external environment, allowing an external water flow to pass through the prototype and collect the heat stored inside it. The exchanger was designed to operate with a relative low water flow, around 1 l per minute, and with a temperature rise not higher than 40 °C between inlet and outlet.

2.2.4 PCM

The choice of the phase change material to be adopted for the prototype was made after a careful analysis of the physical and energy parameters of a series of candidate materials. A first consideration was made regarding the melting and freezing temperature range of the material. For the purpose of this project, in order to make the most of the phase change, the melting temperature should lay around 55°C. This temperature can be easily reached by a solar thermal collector, fully exploiting the phase change latent heat. However, the material must be able to withstand much higher temperatures, which can even reach 100 °C. Moreover, in order to obtain high performances from the thermal point of view, the thermal conductivity, the specific heat and the latent heat should be maximized. Also, some mechanical constraints cannot be neglected and must be respected. For this reason, the density of the material should be as high as possible, so as to ensure a reduced thickness of the storage section. Finally, as in any design choice, the price should be reasonable.

In light of the above, the final choice was to adopt Polyethylene glycol (PEG), with a molecular weight of 6000 g.mol⁻¹, a polyether compound widespread in the medical and chemical industry. The product is marketed in solid-state grains, which solidifies in a single block after the first melting and crystallization cycle, losing the initial granularity. PEG 6000 meets almost all the required characteristics. Its specifications are reported in Table 1.

Table 1. Polyethylene glycol 6000 (PEG6000)

Property	Value	Unit
Melting range	50-55	°C
Melting latent heat	192	kJ.kg ⁻¹

Pre-print version of:

Bilardo, M., Fraisse, G., Pailha, M., & Fabrizio, E. (2019). Design and experimental analysis of an Integral Collector Storage (ICS) prototype for DHW production. *Applied Energy*, 114104.

<https://doi.org/10.1016/j.apenergy.2019.114104>

Specific heat capacity (sensible)	2.3	$\text{kJ.kg}^{-1}.\text{K}^{-1}$
Conductivity	0.2	$\text{W.m}^{-1}.\text{K}^{-1}$
Density (solid)	1210	Kg.m^{-3}
Price (from manufacturer)	~2.8	$\text{€}.\text{kg}^{-1}$

2.3 Test bench and experimental setup

The prototype was installed on a test bench composed of the apparatus itself, the external source of water and all the necessary sensors to study its behaviour. An aluminium structure encloses all the elements and makes the module self-supporting. To support the storage cavity, which is the heaviest element inside the collector, 2 wooden supports have been inserted for each side, in order to thermally decouple the aluminium casing from the storage, avoiding thermal losses. In addition, 2 wooden bars support the cavity on the back, ensuring stability. The entire casing was then fixed to a cement structure positioned at the installation site, to prevent it from moving and guarantee a fixed angle of 33° . Two different installation sites were chosen during the experimental phase. Initially, during summer, the prototype was placed on the ground, inside a solar field predisposed to collecting data. During the winter testing phase, however, it was placed on a flat roof of a neighbouring building. Both sites are located in Bourget-du-Lac (France), inside the university campus of Université Savoie Mont Blanc. This location perfectly recalls the climatic conditions for which the prototype was designed, i.e. a typically cold climate in winter and temperate in summer. The set-up of the test bench was completed by a series of sensors used to monitor the activity of the appliance. 25 K-type thermocouples ($\pm 0.1^\circ\text{C}$ accuracy) were installed in different positions to detect the temperature trend of different parts of the prototype. A flowmeter measures the flow of water that flows inside the DHW exchanger. Solar radiation is finally measured by a pyranometer ($\pm 20 \text{ W.m}^{-2}$ accuracy), while the module of the wind speed is collected using an anemometer. Thermocouples, as well as the flowmeter, were previously calibrated. All data are recorded in an Agilent 34972A acquisition unit (Keysight Technologies) and stored in a USB device. An overview of the prototype test bench is shown in Fig. 11.



Fig. 11. Test bench outdoor installation

Pre-print version of:

Bilardo, M., Fraisse, G., Pailha, M., & Fabrizio, E. (2019). Design and experimental analysis of an Integral Collector Storage (ICS) prototype for DHW production. *Applied Energy*, 114104.

<https://doi.org/10.1016/j.apenergy.2019.114104>

Thermocouples were assembled into two groups, so as to group the cold junctions into two isolated boxes, thus having a uniform reference temperature. Finally, a connection was made to the data acquisition unit, where the potential differences of each individual thermocouple, as well as the reference temperature have been saved. To evaluate the reference temperature a PT100 thermoresistance was used instead of a thermocouple. Fig. 12 illustrates the sensors set up for the experimental data collection.

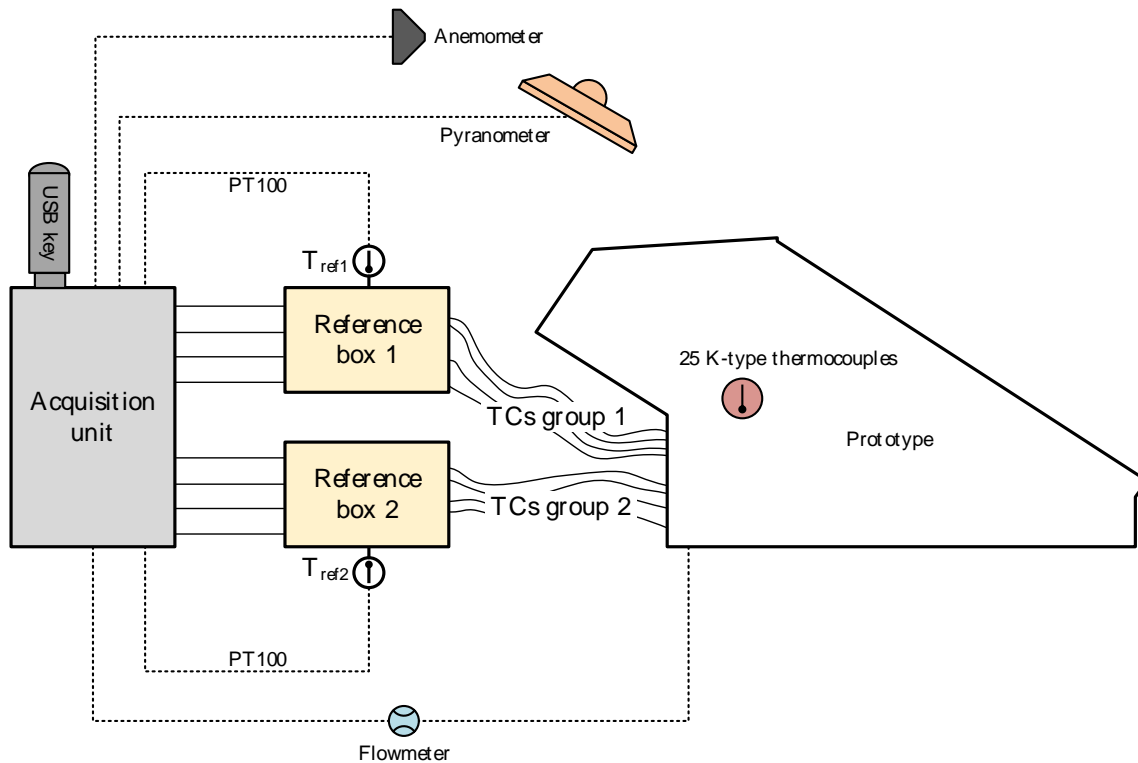


Fig. 12. Bench test set up (sensors detail)

3 Methodology

The experimental study of energy performance, as mentioned in the previous sections, has been divided into two different periods of the year: summer and winter. Similar experimental tests have been carried out to verify the operation of the prototype in both climate conditions and subsequently compare the results. The experimental procedure has been structured into two main assessments. A first preliminary test allowed to study the behaviour of the prototype in preparatory operating conditions, without DHW production: under the effect of solar radiation the device was subjected to heating and cooling cycles, during which the PCM underwent daily phase changes. During this test phase it was also possible to develop some considerations on the overall performances of the

Pre-print version of:

Bilardo, M., Fraisse, G., Pailha, M., & Fabrizio, E. (2019). Design and experimental analysis of an Integral Collector Storage (ICS) prototype for DHW production. *Applied Energy*, 114104. <https://doi.org/10.1016/j.apenergy.2019.114104>

prototype, especially in terms of energy efficiency and solar energy exploitation. The outcomes were compared with data from similar systems already discussed in literature.

A second test phase allowed to test the device during normal operating conditions, with DHW production. For this round of experiments the prototype was connected to the cold-water network. The actual production of DHW was studied performing water collection tests and monitoring the water flow using a ball valve.

The timestep used for data acquisition, which can be adjusted directly from the acquisition unit, was set according to the experimental study performed: during the preparatory operation phases the data were collected every 30 seconds, while during the normal operating tests (DHW production) the acquisition timestep was reduced to 5 seconds, to better visualize the sudden temperature changes within the collector.

3.1 Energy performance parameters

It was necessary to define some physical quantities that could be lately used to evaluate the energy performances of the prototype, so as to make it in some way comparable with other similar systems. Each parameter useful for the analysis of energy performance was evaluated with the same acquisition timestep of the experimental data. The following heat rates have therefore been taken into consideration:

- 1) Heat flux charging the storage

$$\dot{Q}_{sto} = U_{HP} \cdot N_{HP} \cdot \Delta T_{abs/pe} [W] \quad (1)$$

This relation represents the total useful heat flux exchanged between the HP and the storage cavity. U_{HP} represents the heat exchange coefficient of the heat pipe, which was empirically evaluated through an experimental evaluation based on the temperature difference established between the evaporator and condenser. The U_{HP} value was considered constant and set equal to 1.61 WK^{-1} . The overall heat flow is evaluated considering the total number of HP, N_{HP} .

- 2) Heat flux through the HP

$$\dot{Q}_{HP} = U_{HP} \cdot \Delta T_{eva/cond} [W] \quad (2)$$

This quantity represents the amount of heat that passes through a single heat pipe, which depends on the U_{HP} coefficient.

- 3) Heat losses

Pre-print version of:

Bilardo, M., Fraisse, G., Pailha, M., & Fabrizio, E. (2019). Design and experimental analysis of an Integral Collector Storage (ICS) prototype for DHW production. Applied Energy, 114104. <https://doi.org/10.1016/j.apenergy.2019.114104>

$$\dot{Q}_{loss} = D \cdot \Delta T_{pe/ext} [W] \quad (3)$$

This relation estimates the heat rate that is lost by the storage cavity towards the external environment. It is proportional to the temperature difference between the outdoor air and the storage cavity by means of the global thermal loss coefficient D . In order to evaluate the D coefficient value, the prototype was studied in a laboratory environment kept at a constant ambient temperature. After being heated to a temperature of about 63 °C, the storage cavity was left free to cool down until it achieved thermal equilibrium with the environment. The study of the temperature trends during a series of heating and cooling cycles has led to assess the global convective coefficient D equal to 4.42 W.K⁻¹ when the PCM is liquid and 0.82 W.K⁻¹ when it is solid. The detailed study on the global thermal loss coefficient has been carried out in section 3.2.

4) Useful heat flux

$$\dot{Q}_{DHW} = \dot{m}_w \cdot c_{p,w} \cdot \Delta T_{in/out} [W] \quad (4)$$

Actual heat flux extracted by the water flow passing through the DHW exchanger coil. It is proportional to the water temperature difference between the inlet and outlet of the coil by means of the water specific heat ($c_{p,w}$) and water flow rate (\dot{m}_w).

3.2 Evaluation of global heat loss coefficient

This section describes the experimental calculation methodology used to evaluate the global heat loss coefficient D . This coefficient was evaluated on the basis of experimental data and allowed to estimate the heat losses between the storage cavity containing PCM and the external environment, as described by equation (3).

During the whole experiment the prototype was placed in a thermally controlled chamber, whose temperature was kept constant at 21 °C. Through an external heat source, the PCM inside the storage cavity of the prototype was heated up to a temperature of 63 °C, thus achieving the complete melting of the PEG 6000. Subsequently the prototype was left free to cool down inside the thermal chamber, without the interference of external agents, until reaching thermal equilibrium with the surrounding environment. The continuous monitoring of the storage section temperatures allowed to study the cooling process of the prototype. Fig. 13 shows the surface temperature values T_{pe} (cavity frontside), T_{pi} (cavity backside) and T_{ext} (temperature of the thermal chamber) for the duration of the experiment. From the figure it is easy to distinguish the PCM two-phase region, where the phase change takes place, from the liquid and solid phases.

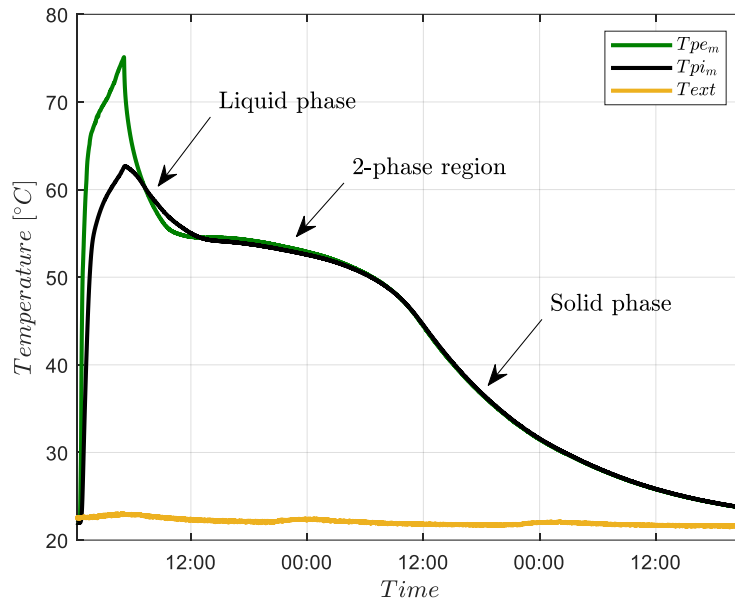


Fig. 13. T_{pe} and T_{pi} temperature trends during natural cooling

After collecting these data, the liquid and solid phases were isolated and studied separately. Applying Newton's law of cooling, fitting curves were obtained for experimental data in the liquid phase (above 55 °C) and solid phase (below 50 °C), according to the differential equation:

$$\begin{cases} \frac{dT}{dt} = -\frac{1}{\tau} \cdot (T - T_{ext}) \\ T(0) = T_0 \end{cases} \quad (5)$$

That gives the following solution:

$$T(t) = T_{ext} + (T_0 - T_{ext}) \cdot e^{-\frac{t}{\tau}} \quad (6)$$

where T_0 is the initial temperature of the cavity and T_{ext} is the temperature of the external environment. τ instead represents the time constant of the system, which can be expressed as:

$$\tau = \frac{C}{D} [s] \quad (7)$$

Where C is the weighted thermal capacity of the prototype components. The value of D , expressed in $W.K^{-1}$, represents the global heat loss coefficient between the cavity and the external environment. Thanks to this analysis, the coefficient D has been used for the future analyses of the experimental data as the main parameter for quantitatively estimating the heat losses of the system. The value of the time constant τ , from which the global convective coefficient D has been evaluated, is different according to whether the PCM is in the liquid or solid phase. For this reason, Newton's law of cooling was applied for both the liquid and solid phases. To assess the numerical value of τ ,

the experimental trend of T_{pe} and T_{pi} was fitted with the exponential function represented by equation (6) (Fig. 14). As a result, two mean values of the global heat loss coefficient D were found, one for the liquid phase D_{liq} (assumed for $T_{PCM} \geq 53 \text{ }^\circ\text{C}$) and one for the solid phase D_{sol} (for $T_{PCM} < 53 \text{ }^\circ\text{C}$):

$$D = \begin{cases} D_{liq} = 4.42 \frac{W}{K} \\ D_{sol} = 0.84 \frac{W}{K} \end{cases} \quad (8)$$

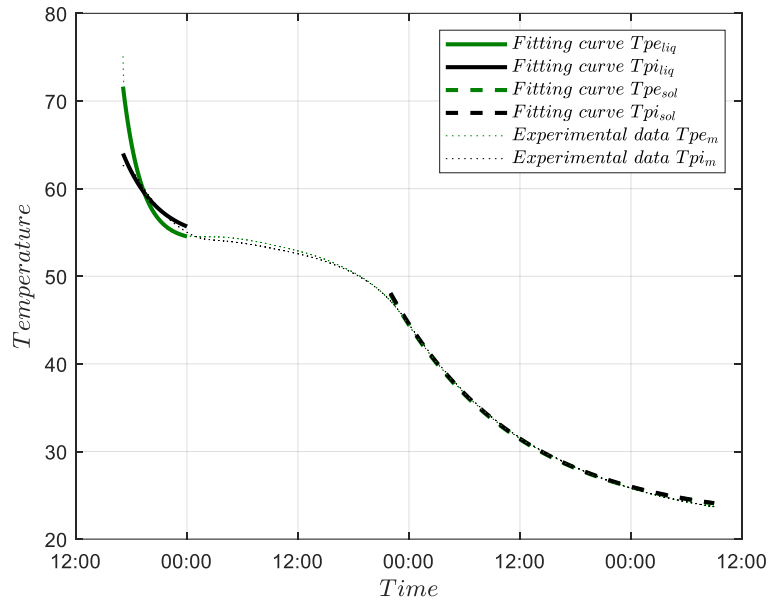


Fig. 14. Exponential fitting for T_{pe} and T_{pi} temperature trends

4 Results

This section presents all the results of the experimental phases set out in section 3. For both the weather conditions selected (summer and winter) the overall performance analysis as well as the DHW production potential were performed. The outcomes are now presented and commented. Table 2 reports a summary of the experiments carried out and their corresponding figures.

Table 2. Experiments summary

	Purpose of the experiment	DHW production / water collection	Season on the experiment	Duration	Corresponding figure
Preparatory operating conditions	General functioning of the prototype	No	Summer	3 days	Fig. 15a
	General functioning of the prototype	No	Winter	3 days	Fig. 15b

	Daily average useful gains versus daily average solar input	No	Summer + Winter	2 months	Fig. 16
	System efficiency	No	Summer + Winter	2 months	Fig. 17
	Energy stored and lost	No	Summer	1 month	Fig. 18a
	Energy stored and lost	No	Winter	1 month	Fig. 18b
Normal operating conditions	General functioning with DHW production	Yes	Summer	1 day	Fig. 20
	Heat flux production	Yes	Summer	1 day	Fig. 21
	General functioning with DHW production	Yes	Winter	1 day	Fig. 22
	Heat flux production	Yes	Winter	1 day	Fig. 23

Initially, the general functioning of the prototype and its internal components was tested. Fig. 15 collects the typical trend of the main temperatures involved in the first experimental study (preparatory operating conditions), with the aim of assessing the correct functioning of the prototype when DHW is not produced. The figure depicts typical summer (Fig. 15a) and winter (Fig. 15b) experimental days, verifying the proper functioning of the test bench. Two different monitoring periods were chosen to verify the behaviour of the prototype in different seasons of the year. All the data presented were collected directly on the experimental site with a 30-second timestep. The trend of the monitored temperatures shows a direct relationship between the solar radiation E (yellow line) and the absorber temperature (blue line). The summer monitored days of study (Fig. 15a) had an undisturbed solar radiation (except for the beginning of day 1), allowing a proper validation of the correct thermal charging process of the storage cavity. Solar radiation reached peak values around 1000 W.m^{-2} , which enabled the absorber to exceed $90 \text{ }^\circ\text{C}$ ($93.4 \text{ }^\circ\text{C}$ max). The temperature of the storage cavity was recorded by four thermocouples positioned on its backside. Their mean value is represented by T_{pi} (black line in the graph). Its trend is clearly shifted with respect to the solar radiation, indicating higher thermal inertia if compared to the absorber. The storage temperature exceeded $70 \text{ }^\circ\text{C}$ every day, growing rather quickly during daylight hours, thanks to solar radiation. However, during night-time, instead of decreasing quickly, the temperature remains stable for several hours around $55 \text{ }^\circ\text{C}$, forming a “plateau” easily recognizable in the graph. That region highlights the process of crystallization of the PCM, during which the solid phase and the liquid phase coexist. This phenomenon does not occur during the day, when the material passes from solid to liquid: the high values of solar radiation make the process of fusion of PCM much faster than that of crystallization, making the phase change less evident. A different behaviour is instead represented in Fig. 15b, showing the data recorded during winter, where the external temperature (T_{ext} , red line)

Pre-print version of:

Bilardo, M., Fraisse, G., Pailha, M., & Fabrizio, E. (2019). Design and experimental analysis of an Integral Collector Storage (ICS) prototype for DHW production. Applied Energy, 114104.

<https://doi.org/10.1016/j.apenergy.2019.114104>

reaches minimum values below 0 °C. In this scenario, the absorber reaches a maximum temperature of 80.5 °C in the hours of higher solar radiation while the temperature of the storage cavity does not exceed 58.1 °C. At this temperature the fusion process of the PCM does not occur and the double phase region is not visible in the graph. However, as will be shown later, the temperature reached is sufficient for DHW production.

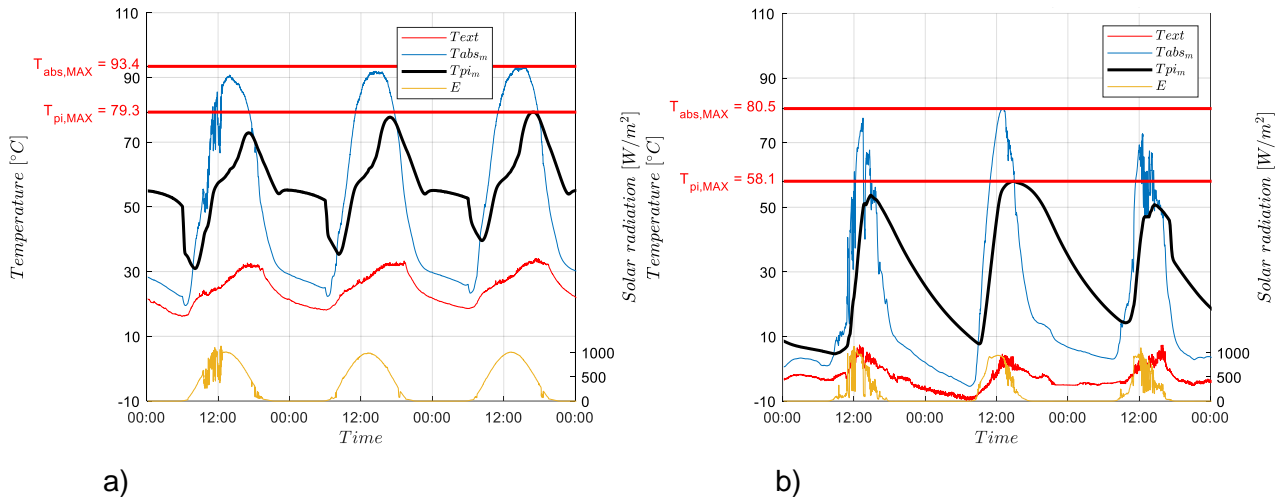


Fig. 15. Main temperatures trends in typical summer (a) and winter (b) experimental days

4.1 Overall performances

The first experimental data collected under the preparatory operation conditions in summer and winter allowed to make some general evaluations on the performance of the prototype. In this analysis, attention has been paid to the ability of the prototype to absorb and store energy within the PCM section. In Fig. 16 the average daily value of the useful gains, as a function of the average daily value of the solar contributions from 9 am to 5 pm, is considered. The result obtained presents the average values evaluated for all the days of the experimental data collection period. To achieve the result shown in the figure, experimental data collected during two months of monitoring, one in summer and one in winter, were considered. A trend line (in red) has been added to the graph, allowing comparison with a similar study conducted by Robinson et al. [31] in which the analysed system was similar to the one under examination, as already reviewed in the state of the art. The analysis shows a result consistent with what is present in the literature, also highlighting a better behaviour of the prototype studied in cases of low solar radiation.

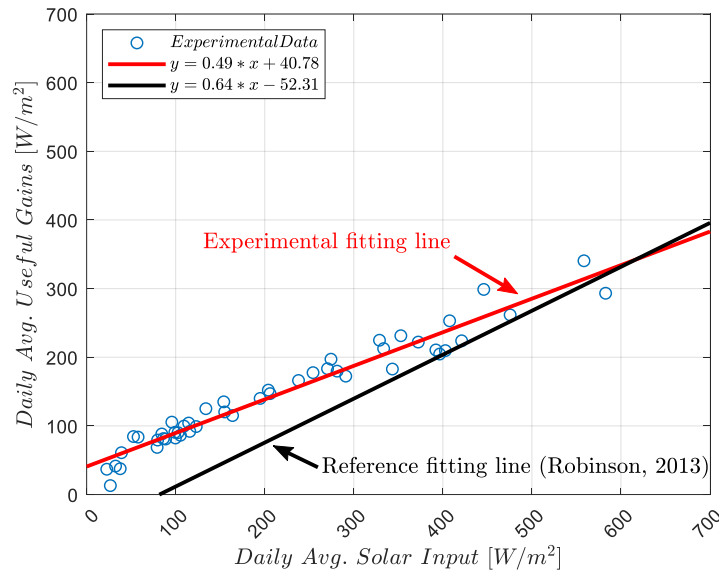


Fig. 16. Daily average useful gains versus daily average solar input from 9 a.m. to 5 p.m.

The mean daily efficiency of the collector was then calculated as the ratio between the heat flux charging the storage \dot{Q}_{sto} and the total solar radiation E , according to the following relation:

$$\eta = \frac{\dot{Q}_{sto}}{E \cdot A_{abs}} = \frac{U_{HP} \cdot N_{HP} \cdot (T_{abs} - T_{pe})}{E \cdot A_{abs}} [-] \quad (9)$$

The average efficiency values for each day are collected in Fig. 17 as a function of the temperature difference between storage and external environment over solar radiation. Each value in the figure (blue circles) represents an experimental day for the periods considered (a winter month and a summer month). Using the previous approach a linear trendline was drawn (solid red line), demonstrating that the system achieves an efficiency of 61.0% when the storage temperature is equal to the external one. As in Fig. 16, the fitting line found by Robinson et al. [31] in his study has been reported, showing once again the affinity between the two systems.

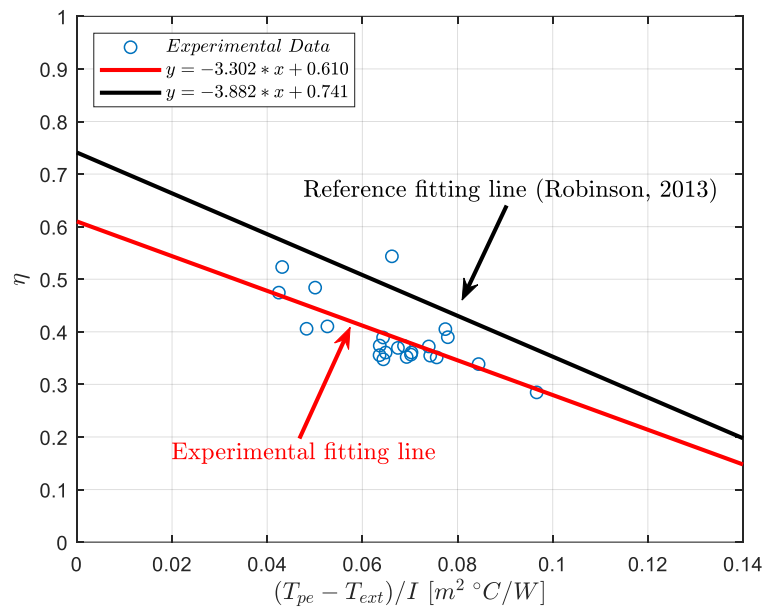
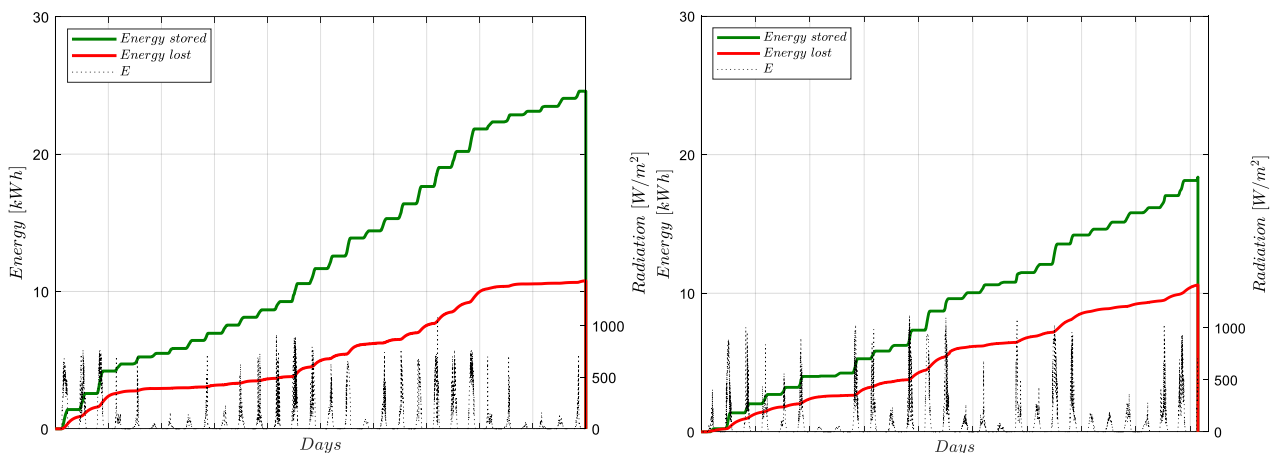


Fig. 17. System efficiency versus loss potential/insulation ratio

What emerges from this analysis is certainly a poor optical efficiency of the collector, which is rather low compared to similar collectors with heat pipes studied in the literature [47]. The glazed surface installed in the prototype is in fact a standard cover glass, with poor optical and thermal performance. Furthermore, the reference fitting line described by Robinson [31] lead to better efficiency. This result is due to a different definition of the efficiency η , that in Robinson’s study also accounts the thermal losses toward the conditioned environment.

In the same preliminary test phase, heat losses were also considered, by evaluating the energy stored during two typical months of the studied periods and comparing it with the energy lost during the same periods. The results are collected in Fig. 18a (summer month) and Fig. 18b (winter month). Both the energy lost and stored are expressed in kWh. After being integrated over time, equations (1) and (3) were used for this analysis and the values refer to the single prototype, with an absorption area of 0.5 m².



a) b)

Fig. 18. Energy stored and energy lost in a typical summer (a) and winter (b) month

What comes out from the graphs is a significant impact of thermal losses on the thermal storage capacity of the prototype, regardless of the period considered. As expected, solar radiation (black dashed line) has a considerable influence on the stored energy: the higher the solar activity, the higher the amount of energy stored. On the contrary, thermal losses are affected too: intense solar activity in this case seem to induce higher energy losses. Overall, the total amount of thermal energy stored within the cavity reaches 24.57 kWh in the summer monitored month and 18.16 kWh in the winter month.

A positive thermal effect achieved by the prototype is the maintenance of the temperature in the cavity in a secure range for the system operation. Fig. 19 shows the temperature difference between the PCM cavity (T_{pi}) and the external air (T_{ext}) as a function of the external air temperature (T_{ext}), both for the summer (a) and winter (b) months. The graph shows how the difference between T_{pi} and T_{ext} never exceeds 50 °C in summer, avoiding an overheating risk of the material (with possible degradation phenomena). During the winter month, the monitored temperature difference is always above 5 °C, avoiding the risk of water freezing inside the system.

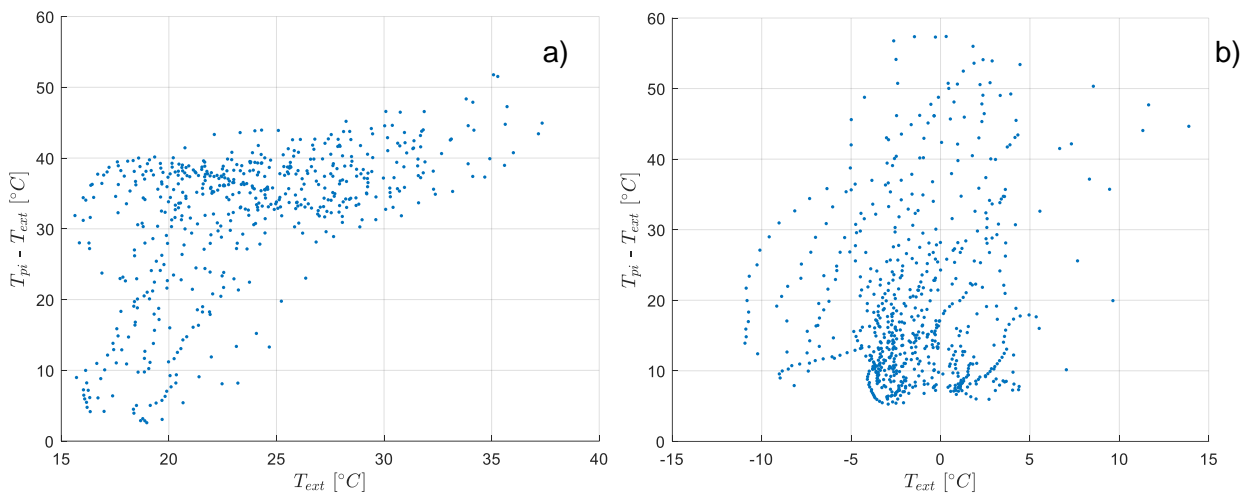


Fig. 19. Temperature difference between PCM cavity and outdoor air as a function of the outdoor temperature in a typical summer (a) and winter (b) month

4.2 DHW production

DHW productivity was the focus of the second experimental test. The production of DHW was tested both during summer and winter. During the test period performed in summer two water collection moments were scheduled: at 12:00 for 15 minutes and at 17:00 for a duration of 30 minutes. Productivity has been studied by running a cold-water flow directly coming from the water network, at an average temperature of about 13 °C, and measuring the temperature rise that the

Pre-print version of:

Bilardo, M., Fraisse, G., Pailha, M., & Fabrizio, E. (2019). Design and experimental analysis of an Integral Collector Storage (ICS) prototype for DHW production. *Applied Energy*, 114104.

<https://doi.org/10.1016/j.apenergy.2019.114104>

water flow underwent by passing through the heat exchanger inside the prototype. For this experiment a water flow equal to $1.82 \text{ l}\cdot\text{min}^{-1}$ was set for the first water collection, and then decreased down to $0.87 \text{ l}\cdot\text{min}^{-1}$ for the second collection. The two collection moments are reported in Fig. 20 where the solid black line referred to the right axes represent the water flow of DHW produced. The purpose of this phase was to investigate the thermal power that the prototype is able to provide to a possible user. Fig. 20 examines a typical experimental day of the summer period, highlighting the temperature trend of the storage cavity and the water collected. The temperature difference between the front surface of the cavity (green line) and the back surface (black line) never exceeds $10 \text{ }^\circ\text{C}$, indicating an effective heat exchange inside the honeycomb structure. Furthermore, the temperature of the front plate (T_{pe}) is higher during the day, thanks to the effect of solar radiation. At night, instead, the back plate (T_{pi}), dissipating less heat, is at a higher temperature. The temperature of the water leaving the heat exchanger almost reached $50 \text{ }^\circ\text{C}$, without decreasing below $30 \text{ }^\circ\text{C}$ for the entire duration of the collection. What can be noted in the picture is the effect that the water collection has on the cavity. The first collection moment, carried out at around 12:00, has a significant impact on cavity temperatures, whereas the second, performed at 17:00, affects the cavity much less. Besides the flow rate difference, this behaviour can be justified by the fact that at 12:00 the PCM in the cavity, having a temperature slightly above $50 \text{ }^\circ\text{C}$, had not yet reached the total liquid phase and consequently the latent heat accumulated was not fully exploited. On the contrary, by the time of the second collection of water, as the cavity temperature was above $60 \text{ }^\circ\text{C}$, it was possible to exploit the latent heat accumulated in the PCM. This explains why the two water samples have a very different impact on the temperature of the cavity, which drastically decreases only in the first collection. It is also easy to notice how the front plate of the cavity, being in direct contact with the water heat exchanger, is more affected by temperature variations. The correlation between the outlet temperature and the PCM temperature is interesting because it proves that the latent heat of the PCM is properly exploited. This is a rather remarkable outcome, since it allows to produce DHW without significantly affecting the storage temperature, as it happens in classic solar collectors coupled with sensible-heat storages. In addition to this, the cavity temperature rise up to $55 \text{ }^\circ\text{C}$ at the beginning of the day is rapid due to the lower specific heat capacity of the PCM solid phase in comparison with standard water-based storage. This results in lower backup energy consumption for charging the thermal storage.

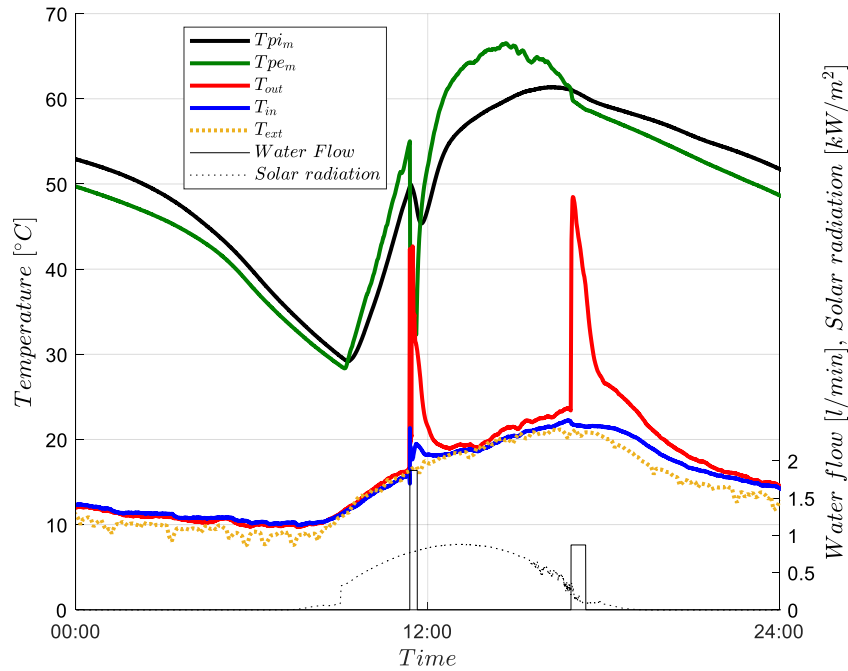


Fig. 20. Water collection experiment in summer condition

Focusing on the second water collection moment (around 17:00), the instantaneous power extracted from the water during the experiment was evaluated in Fig. 21. An average value of 1.32 kW was determined as shown by the solid red line in the figure. The prototype was therefore able to supply a specific heat flux of about $2.64 \text{ kW}\cdot\text{m}^{-2}$, with a water flow equal to $0.87 \text{ l}\cdot\text{min}^{-1}$.

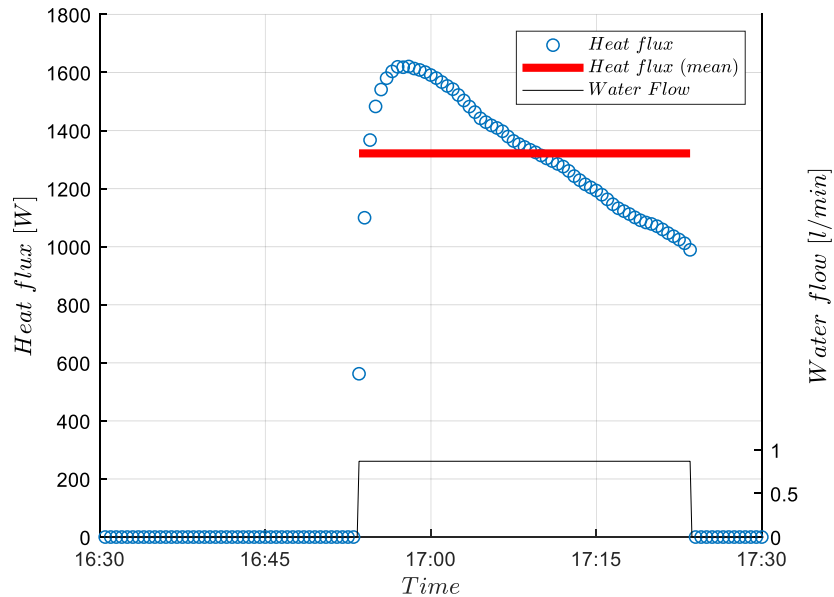


Fig. 21. Extracted heat flux in summer condition

The same experimental approach was carried out for the winter period, confirming the results already obtained. However, in this second experimental phase, depicted in Fig. 22, a single water collection was performed after 17:00, for a total duration of about 20 minutes. Since the sampling was carried out in harsh climatic conditions, that time of day was selected to let the storage cavity reach an average temperature above 45 °C. The flow of water used was variable, initially equal to 1.82 l.min⁻¹, and then decreased to 0.87 l.min⁻¹. Given the low temperature at which the PCM was stored, the water at the outlet of the exchange coil reached the initial temperature of 35 °C, and then decreased to 25 °C. Also in this case the impact of the water collection is considerable on the front surface of the cavity, which undergoes a drastic decrease in temperature (green line).

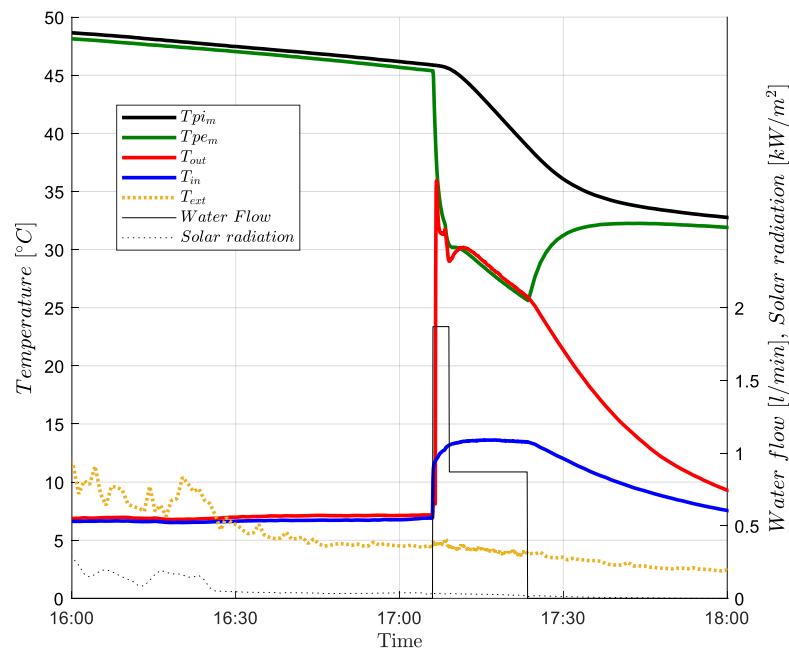


Fig. 22. Water collection experiment in winter condition

Finally, in Fig. 23 the useful heat flux was evaluated. The water collection was characterized by an average heat flux value of 881 W (red line). The specific heat flux reached can therefore be considered equal to 1.76 kW.m⁻².

Pre-print version of:

Bilardo, M., Fraisse, G., Pailha, M., & Fabrizio, E. (2019). Design and experimental analysis of an Integral Collector Storage (ICS) prototype for DHW production. *Applied Energy*, 114104.

<https://doi.org/10.1016/j.apenergy.2019.114104>

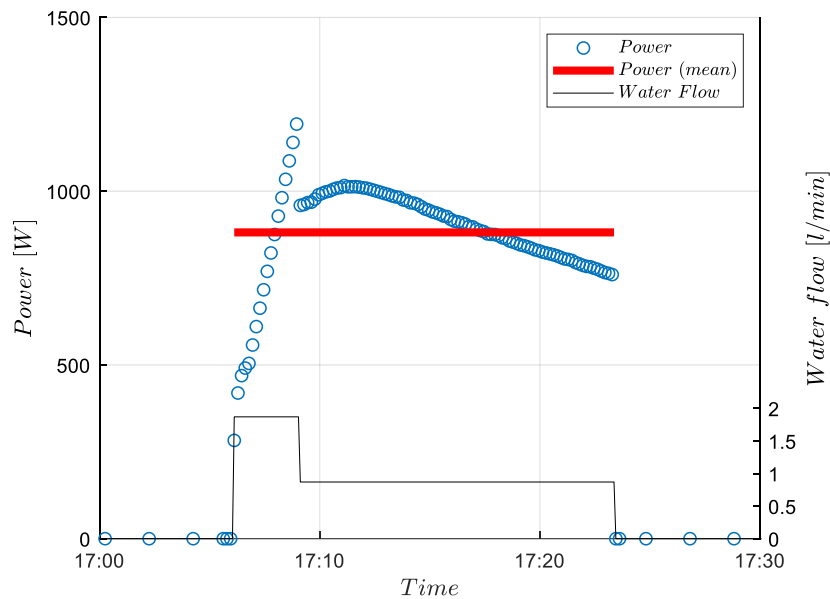


Fig. 23. Extracted heat flux in winter condition

5 Conclusions

This paper analysed an innovative ICS prototype for DHW production. An accurate description of the internal components allowed to characterization of the prototype and the description of its operating principle. A careful review of similar systems shows that this ICS prototype is unique in its kind. The characteristic that distinguishes it is the coupling of heat pipes with a phase change material (PCM) storage section. Both heat pipes and PCM storage are assembled ad hoc in a single, specially insulated casing. The device may therefore be placed in the category of passive solar systems with integrated storage, not requiring external auxiliary energy to operate. In particular, the prototype was designed to ensure easy architectural integration, especially considering its reduced absorbent surface, equal to 0.5 m^2 . Furthermore, a meticulous design and positioning of the insulating material make this device suitable for harsh climatic conditions.

The energy performances of the prototype were tested during the summer and winter months. A first set of experiments ensured the correct operation of the machine. Subsequently, the thermal storage capacity and DHW productivity were evaluated. The results obtained confirmed what was expected from the design phase. The prototype was able to accumulate a monthly thermal energy of 24.57 kWh in the summer monitored month. The production power of DHW, on the other hand, ranged from $1.76 \text{ kW}\cdot\text{m}^{-2}$ to $2.64 \text{ kW}\cdot\text{m}^{-2}$ depending on the experimental conditions tested. The heat storage capacity was studied, demonstrating how the prototype is able to reach high thermal levels in reduced times (lower specific heat capacity compared to water storage systems) without compromising the energy density of the storage (latent heat exploitation). With the designed system,

Pre-print version of:

Bilardo, M., Fraisse, G., Pailha, M., & Fabrizio, E. (2019). Design and experimental analysis of an Integral Collector Storage (ICS) prototype for DHW production. *Applied Energy*, 114104. <https://doi.org/10.1016/j.apenergy.2019.114104>

the cavity is always kept below dangerous overheating temperatures in summer, avoiding PMC degradation. On the other hand, the insulated envelope avoids the risk of water freezing inside the system, keeping the cavity temperature always higher than the water freezing point.

The results of this investigation show that the studied prototype offers similar energy performance compared to traditional systems available on the market. However, the findings of the study demonstrated the high prospective for this new concept of ICS. This study offers insight into the coupling between heat pipes and PCM that until now had never been implemented together within a solar collector. Although the current study is based on a relatively small prototype, the findings suggest that the potential of this technology is certainly promising. Further research should be undertaken to explore how the use of several of these prototypes in parallel can satisfy the energy needs of real users.

The experimental analysis contained in this study supported the development of a numerical model able to describe the functioning of the prototype. Thanks to the experimental data collected and presented in this paper, the model was calibrated and validated [43]. The energy performances of the prototype were simulated to meet a DHW demand of a typical small residential user equal to 200 l.day⁻¹. Based on this requirement, an average annual solar fraction of 56% was reached with a total absorbent surface of 3 m² (equivalent to 6 prototypes).

Acknowledgements

This study has been supported and funded by the “Agence de l’Environnement et de la Maitrise de l’Energie” (ADEME), under grant agreement N° 1205C0129. Partners: LOCIE, INSULA, SMCI, DATE.

References

- [1] REN21, *Renewables 2018: Global Status Report*, 2018.
- [2] IEA, *Global Energy & CO₂ Status Report*, 2018. <http://www.iea.org/publications/freepublications/publication/GECO2017.pdf>.
- [3] European Union, *DIRECTIVE 2009/28/EC OF THE EUROPEAN PARLIAMENT AND OF THE COUNCIL on the promotion of the use of energy from renewable sources and amending and subsequently repealing Directives 2001/77/EC and 2003/30/EC*, 2009. <https://eur-lex.europa.eu/legal-content/EN/TXT/PDF/?uri=CELEX:32009L0028&from=EN> (accessed December 17, 2018).
- [4] P. Capros, N. Tasios, A. De Vita, L. Mantzos, L. Parousos, *Technical report accompanying the analysis of options to move beyond 20% GHG emission reduction in the EU by 2020: Member State results*, 2012. https://ec.europa.eu/clima/sites/clima/files/strategies/2020/docs/technical_report_analysis_2012_en.pdf (accessed December 17, 2018).
- [5] REN21, *Renewable 2014: Global Status Report*, 2014.

Pre-print version of:

Bilardo, M., Fraisse, G., Pailha, M., & Fabrizio, E. (2019). Design and experimental analysis of an Integral Collector Storage (ICS) prototype for DHW production. *Applied Energy*, 114104.

<https://doi.org/10.1016/j.apenergy.2019.114104>

http://www.ren21.net/Portals/0/documents/Resources/GSR/2014/GSR2014_full_report_low_res.pdf.

- [6] C. Robinson, B. Dilkina, J. Hubbs, W. Zhang, S. Guhathakurta, M.A. Brown, R.M. Pendyala, Machine learning approaches for estimating commercial building energy consumption, *Appl. Energy*. (2017). doi:10.1016/j.apenergy.2017.09.060.
- [7] Ministère de l'Égalité des Territoires et du Logement, Réglementation thermique 2012, version modifiée avril 2013, *J. Off. La République Française*. (2013) 12. <http://www.legifrance.gouv.fr> (accessed October 19, 2018).
- [8] Gazzetta Ufficiale della Repubblica Italiana, Attuazione della direttiva 2009/28/CE sulla promozione dell'uso dell'energia da fonti rinnovabili, recante modi ca e successiva abrogazione delle direttive 2001/77/CE e 2003/30/CE, 2011. <http://unmig.sviluppoeconomico.gov.it/unmig/norme/pdf/28dlg11.pdf> (accessed December 17, 2018).
- [9] European Union, Directive (EU) 2018/ of the European Parliament and of the Council of 30 May 2018 amending Directive 2010/31/EU on the energy performance of buildings and Directive 2012/27/EU on energy efficiency, *Off. J. Eur. Union*. 2018 (2018) 75–91. <https://eur-lex.europa.eu/legal-content/EN/TXT/PDF/?uri=CELEX:32018L0844&from=EN> (accessed October 16, 2018).
- [10] F. Ascione, R.F. De Masi, F. de Rossi, S. Ruggiero, G.P. Vanoli, Optimization of building envelope design for nZEBs in Mediterranean climate: Performance analysis of residential case study, *Appl. Energy*. (2016). doi:10.1016/j.apenergy.2016.09.027.
- [11] M. Ferrara, E. Fabrizio, J. Virgone, M. Filippi, A simulation-based optimization method for cost-optimal analysis of nearly Zero Energy Buildings, *Energy Build.* 84 (2014) 442–457. doi:10.1016/j.enbuild.2014.08.031.
- [12] M. Ferrara, E. Sirombo, A. Monti, E. Fabrizio, M. Filippi, Influence of envelope design in the optimization of the operational energy costs of a multi-family building, *Energy Procedia*. 101 (2016) 216–223. doi:10.1016/j.egypro.2016.11.028.
- [13] Y. Zhang, P.E. Campana, Y. Yang, B. Stridh, A. Lundblad, J. Yan, Energy flexibility from the consumer: Integrating local electricity and heat supplies in a building, *Appl. Energy*. (2018). doi:10.1016/j.apenergy.2018.04.041.
- [14] D. Hailot, E. Franquet, S. Gibout, J.-P. Bédécarrats, Optimization of solar DHW system including PCM media, *Appl. Energy*. 109 (2013) 470–475. doi:10.1016/J.APENERGY.2012.09.062.
- [15] F. Mauthner, W. Weiss, M. Spörk-Dür, Solar Heat Worldwide: Markets and Contribution to the Energy Supply 2014, (2016) 76.
- [16] W. Weiss, M. Spörk-Dür, Solar Heat Worldwide: Global Market Development and Trends in 2017, 2018.
- [17] Grand View Research, Thermal Energy Storage Market Analysis By Type (Sensible Heat Storage, Latent Heat Storage, Thermochemical Heat Storage), By Technology, By Storage Material, By Application, By End-use, And Segment Forecasts, 2018 - 2025, 2017. <https://www.grandviewresearch.com/industry-analysis/thermal-energy-storage-market> (accessed December 17, 2018).
- [18] A. Arteconi, N.J. Hewitt, F. Polonara, State of the art of thermal storage for demand-side management, *Appl. Energy*. 93 (2012) 371–389. doi:10.1016/J.APENERGY.2011.12.045.
- [19] U.S. Department of Energy, Demand Response and Energy Storage Integration Study, 2016. <https://www.energy.gov/sites/prod/files/2016/03/f30/DOE-EE-1282.pdf> (accessed December 17, 2018).
- [20] A. Dahash, F. Ochs, M.B. Janetti, W. Streicher, Advances in seasonal thermal energy storage for solar district heating applications: A critical review on large-scale hot-water tank and pit

Pre-print version of:

Bilardo, M., Fraisse, G., Pailha, M., & Fabrizio, E. (2019). Design and experimental analysis of an Integral Collector Storage (ICS) prototype for DHW production. *Applied Energy*, 114104.

<https://doi.org/10.1016/j.apenergy.2019.114104>

- thermal energy storage systems, *Appl. Energy*. 239 (2019) 296–315. doi:10.1016/J.APENERGY.2019.01.189.
- [21] Z. Ma, H. Bao, A.P. Roskilly, Seasonal solar thermal energy storage using thermochemical sorption in domestic dwellings in the UK, *Energy*. 166 (2019) 213–222. doi:10.1016/j.energy.2018.10.066.
- [22] R. Elbahjaoui, H. El Qarnia, Performance evaluation of a solar thermal energy storage system using nanoparticle-enhanced phase change material, *Int. J. Hydrogen Energy*. 44 (2019) 2013–2028. doi:10.1016/j.ijhydene.2018.11.116.
- [23] Y. Tian, C.-Y.Y. Zhao, A review of solar collectors and thermal energy storage in solar thermal applications, *Appl. Energy*. 104 (2013) 538–553. doi:10.1016/j.apenergy.2012.11.051.
- [24] S.M. Hasnain, Review on sustainable thermal energy storage technologies, part I: heat storage materials and techniques, n.d. https://ac.els-cdn.com/S0196890498000259/1-s2.0-S0196890498000259-main.pdf?_tid=c76f3825-4ce4-4ebb-b03d-60a59b5ee5d7&acdnat=1547725681_1566fb5b7dc521936da44e603120640a (accessed January 17, 2019).
- [25] K. Du, J. Calautit, Z. Wang, Y. Wu, H. Liu, A review of the applications of phase change materials in cooling, heating and power generation in different temperature ranges, *Appl. Energy*. 220 (2018) 242–273. doi:10.1016/J.APENERGY.2018.03.005.
- [26] E. and I.S. Department for Business, Evidence Gathering: Thermal Energy Storage (TES) Technologies, 2016. https://www.gov.uk/government/uploads/system/uploads/attachment_data/file/545249/DELT_A_EE_DECC_TES_Final__1_.pdf.
- [27] K. Nithyanandam, R. Pitchumani, Design of a latent thermal energy storage system with embedded heat pipes, *Appl. Energy*. 126 (2014) 266–280. doi:10.1016/J.APENERGY.2014.03.025.
- [28] K. Chopra, V.V. Tyagi, A.K. Pandey, A. Sari, Global advancement on experimental and thermal analysis of evacuated tube collector with and without heat pipe systems and possible applications, *Appl. Energy*. 228 (2018) 351–389. doi:10.1016/J.APENERGY.2018.06.067.
- [29] M. Smyth, P.C. Eames, B. Norton, Integrated collector storage solar water heaters, *Renew. Sustain. Energy Rev.* 10 (2006) 503–538. doi:10.1016/j.rser.2004.11.001.
- [30] N. Susheela, M.K. Sharp, Heat Pipe Augmented Passive Solar System for Heating of Buildings, *J. Energy Eng.* 127 (2001) 18–36. doi:10.1061/(ASCE)0733-9402(2001)127:1(18).
- [31] B.S. Robinson, N.E. Chmielewski, A. Knox-Kelecy, E.G. Brehob, M.K. Sharp, Heating season performance of a full-scale heat pipe assisted solar wall, *Sol. Energy*. 87 (2013) 76–83. doi:10.1016/j.solener.2012.10.008.
- [32] B.S. Robinson, M.K. Sharp, Reducing unwanted thermal gains during the cooling season for a solar heat pipe system, *Sol. Energy*. 115 (2015) 16–32. doi:10.1016/j.solener.2015.02.011.
- [33] M. Esen, H. Esen, Experimental investigation of a two-phase closed thermosyphon solar water heater, *Sol. Energy*. 79 (2005) 459–468. doi:10.1016/j.solener.2005.01.001.
- [34] J. Prakash, D. Roan, W. Tauqir, H. Nazir, M. Ali, A. Kannan, Off-grid solar thermal water heating system using phase-change materials: design, integration and real environment investigation, *Appl. Energy*. (2019). doi:10.1016/j.apenergy.2019.02.058.
- [35] S. Sadhishkumar, T. Balusamy, Performance improvement in solar water heating systems - A review, *Renew. Sustain. Energy Rev.* 37 (2014) 191–198. doi:10.1016/j.rser.2014.04.072.
- [36] D. Vikram, S. Kaushik, V. Prashanth, N. Nallusamy, An Improvement in the Solar Water Heating Systems by Thermal Storage Using Phase Change Materials, in: *Sol. Energy*, ASME, 2006: pp. 409–416. doi:10.1115/ISEC2006-99090.
- [37] A. Shukla, D. Buddhi, R.L. Sawhney, Solar water heaters with phase change material thermal energy storage medium: A review, (n.d.). doi:10.1016/j.rser.2009.01.024.

Pre-print version of:

Bilardo, M., Fraisse, G., Pailha, M., & Fabrizio, E. (2019). Design and experimental analysis of an Integral Collector Storage (ICS) prototype for DHW production. *Applied Energy*, 114104.

<https://doi.org/10.1016/j.apenergy.2019.114104>

- [38] T. Kousksou, P. Bruel, G. Cherreau, V. Leoussoff, T. El Rhafiki, PCM storage for solar DHW: From an unfulfilled promise to a real benefit, *Sol. Energy*. 85 (2011) 2033–2040. doi:10.1016/j.solener.2011.05.012.
- [39] G. Serale, E. Fabrizio, M. Perino, Design of a low-temperature solar heating system based on a slurry Phase Change Material (PCS), *Energy Build.* 106 (2015) 44–58. doi:10.1016/j.enbuild.2015.06.063.
- [40] D. Haillot, V. Goetz, X. Py, M. Benabdelkarim, High performance storage composite for the enhancement of solar domestic hot water systems. Part 1: Storage material investigation, *Sol. Energy*. 85 (2011) 1021–1027. doi:10.1016/j.solener.2011.02.016.
- [41] D. Haillot, F. Nepveu, V. Goetz, X. Py, M. Benabdelkarim, High performance storage composite for the enhancement of solar domestic hot water systems. Part 2: Numerical system analysis, *Sol. Energy*. 86 (2012) 64–77. doi:10.1016/j.solener.2011.09.006.
- [42] J.V.D. Souza, G. Fraisse, M. Pailha, S. Xin, Experimental study of a partially heated cavity of an integrated collector storage solar water heater (ICSSWH), *Sol. Energy*. 101 (2014) 53–62. doi:10.1016/j.solener.2013.11.023.
- [43] M. Bilardo, G. Fraisse, M. Pailha, E. Fabrizio, Modelling and performance analysis of a new concept of integral collector storage (ICS) with phase change material, *Sol. Energy*. 183 (2019) 425–440. doi:10.1016/J.SOLENER.2019.03.032.
- [44] M. Héder, From NASA to EU: The evolution of the TRL scale in Public Sector Innovation, *Innov. J.* 22 (2017) 1–23.
- [45] CLIPSOL, Capteur Solaire Thermique Clipsol, (n.d.). https://www.sav.clipsol.com/boutique/liste_familles.cfm?num=51&code_lg=lg_fr (accessed May 13, 2019).
- [46] G. Fraisse, M. Pailha, Etude numérique et expérimentale d'un nouveau concept de capteur solaire thermique auto-stockeur à changement de phase, in: *Journées Natl. Sur l'Energie Sol.*, 2016.
- [47] A. Shafieian, M. Khiadani, A. Nosrati, A review of latest developments, progress, and applications of heat pipe solar collectors, *Renew. Sustain. Energy Rev.* 95 (2018) 273–304. doi:10.1016/J.RSER.2018.07.014.